Coulomb instability of multicharged proteins

Joshua Jortner *, Isidore Last, Yaacov Levy [1]

School of Chemistry, Tel Aviv University, Ramat Aviv, Tel Aviv 69978, Israel

Abstract

We studied the energetics and fragmentation patterns of multicharged $(A^+)_n$ Morse clusters ($n = 55$–321), with a total cluster charge $Z = n$. The Morse pair-potential parameters were characterized by the dissociation energy $D = 1$–10 eV, range parameter $\alpha = 1$–3 Å^{-1}, and interatomic equilibrium separation $R_e = 1$–3 Å. The potential energies ε (per particle) of these multicharged Morse clusters at their equilibrium configuration (with bond length r_0) were analyzed in terms of the liquid drop model. This resulted in the relation $\varepsilon = (\bar{a}_C^0/r_0)n^{2/3} + (\bar{a}_v^0 D/\alpha r_0) + [\bar{a}_s^0 D/(\alpha r_0)^{3/2}]n^{-1/3}$, where the reduced parameters $\bar{a}_C^0$ (for the Coulomb energy), $\bar{a}_v^0$ (for the interior energy) and $\bar{a}_s^0$ (for the surface energy) are independent of the Morse pair-potential parameters. The Rayleigh fissibility parameter $X = E(\text{Coulomb})/2E(\text{surface})$, which determines the fragmentation pattern (i.e., $X < 1$ for cluster fission and $X > 1$ for Coulomb explosion), was expressed in the form $X = (Z^2/n)[(2\bar{a}_s^0/\bar{a}_C^0)(D/\alpha^{3/2}r_0^{1/2})]^{-1}$. The application of this result to the Coulomb instability of multicharged globular proteins reveals that $X < 1$ for the currently available data. The dominating fragmentation channel is expected to involve spatially anisotropic protein fission into a small number of large fragments, rather than spatially isotropic protein Coulomb explosion into a large number of small fragments.
© 2006 Elsevier B.V. All rights reserved.

Keywords: Coulomb explosion; Morse cluster; Liquid drop model; Multicharged protein

1. Introduction

The fragmentation of multiply charged clusters driven by long-range Coulomb forces [1–50] bears close analogy to Coulomb instability of nuclei [51–54], droplets [55–58], and pseudo-Coulomb instability of optical molasses [59,60]. These large, finite, multicharged (or effectively charged) systems span a broad size domain of 10–12 orders of magnitude, from femtometer structures of nuclei [51–54] to nanometer structures of large molecules and clusters, to micrometer structures of irradiated ultracold gases [59,60], and to millimeter structures of droplets [56–58]. In general, Coulomb instability is due to repulsion between positive charges. In this context some interesting questions arise regarding the energetics and dynamics of the fragmentation patterns of multicharged finite systems:

(1) How does a finite system respond to a large excess charge?

(2) What are the topography and topology of the multidimensional energy landscape that guides the system's fragmentation dynamics?

(3) What are the fragmentation channels and under what conditions are they realized?

(4) What is the interplay between fission, i.e., instability towards dissociation of the multicharged finite system into two (or a small number of) large fragments and Coulomb explosion into a large number of small ionic species?

In our previous studies [48,49] we addressed unifying features of fragmentation channels driven by long-range Coulomb forces in clusters, nuclei and droplets. We studied the energetics, fragmentation patterns and dynamics of multicharged $(A^+)_n$ ($n = 55$, 135, 321) Morse clusters. The variation of the range of the pair-potential induced changes in the cluster surface energy and in the Rayleigh fissibility parameter [55,10,21, 48,49]

$$X = E(\text{Coulomb})/2E(\text{surface}) \tag{1}$$

where $E(\text{Coulomb})$ is the cluster Coulomb energy and $E(\text{surface})$ is the cluster surface energy. Molecular dynamics simulations [48,49] established two distinct fragmentation patterns of

* Corresponding author. Tel.: +972 3 6408322; fax: +972 3 6415054.
  E-mail address: jortner@chemsg1.tau.ac.il (J. Jortner).
[1] Present address: Department of Physics, 6230 Urey Hall, University of California, San Diego, 9500 Gilman Drive, La Jolla, CA 92093-0371, USA.
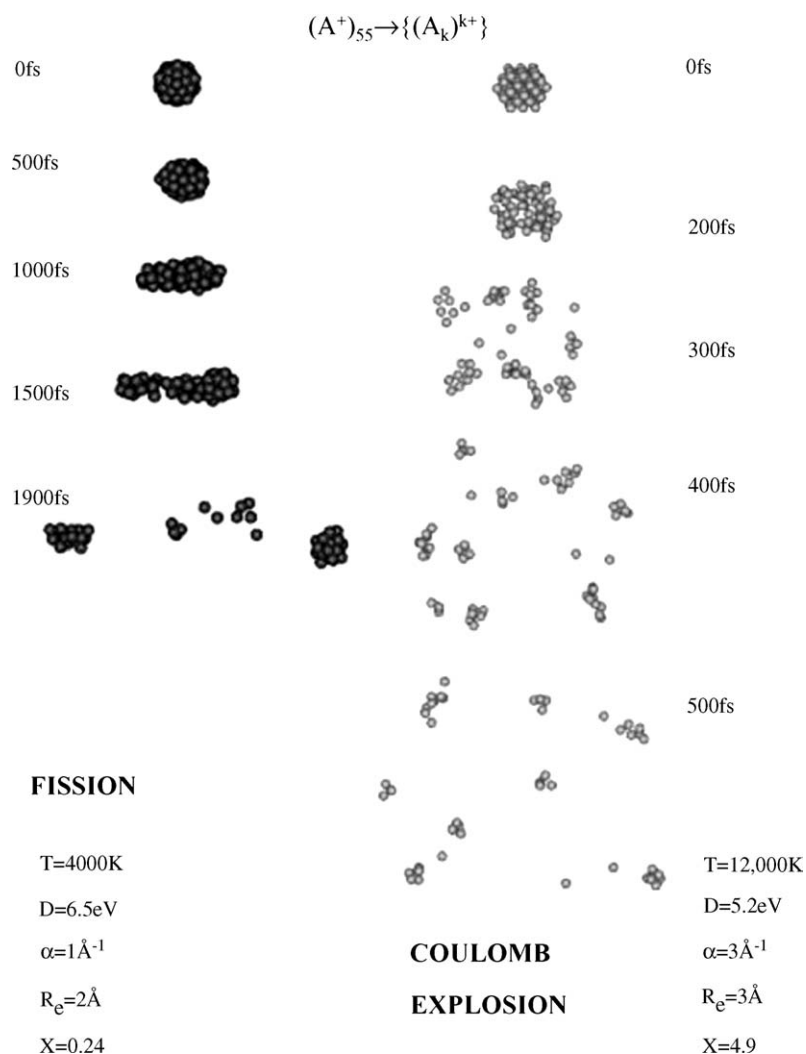
Fig. 1. Snapshots of the time-resolved fragmentation dynamics of highly charged $(A^+)_{55}$ Morse clusters. The potential parameters are marked on the two panels. The right panel corresponds to an (s) Morse pair potential with the Rayleigh fissibility parameter $X = 4.9$. The left panel corresponds to a (ℓ) Morse pair-potential interaction with $X = 0.24$. The mass of each A^+ ion is 100 amu, its charge is $q = 1$ and the total cluster charge is $Z = n$. The Morse pair-potential parameters, Eqs. (2) and (3), are marked on each panel. The transient structures at different times ($t = 0$–1500 fs) are marked on each picture. Data adopted from Ref. [49]. Note the dramatic distinction between the spatially isotropic Coulomb explosion in the right panel and the spatially anisotropic fission in the left panel.

multicharged clusters that involve spatially anisotropic cluster fission into a small number of large, multicharged clusters for $X < 1$, and spatially isotropic Coulomb explosion into a large number of individual ions and small ionic fragments for $X > 1$ (Fig. 1). The Rayleigh instability limit $X = 1$ separates between spatially anisotropic fission and spatially isotropic Coulomb explosion [48,49]. The energetics of the ionic fragments is also qualitatively different for the two fragmentation channels, where for fission both the fragments' total kinetic energy E_{KIN} and their inner energy E_{IN} are high, with $E_{KIN}/E_{IN} \sim 1$, while for Coulomb explosion $E_{KIN}/E_{IN} \gg 1$. We also explored [50] the fission and Coulomb explosion fragmentation dynamics of multicharged $(A^+)_{55}$ Morse clusters. The multidimensional energy landscapes for these fragmentation processes were explored by constructing reduced coordinates utilizing the principal component analysis, which was previously applied for the energy landscapes and folding dynamics of biomolecules. The distance-

matrix based principal component analysis was applied [50] to study the effects of the potential on the fragmentation dynamics and to explore the structural diversity of the fragmentation processes.

In the realm of biophysics, highly charged peptides and proteins were interrogated by mass spectrometry [61,62], providing significant information on the structure, reactivity, conformational changes and folding of "isolated" anhydrous proteins [61,62]. It is interesting to inquire what the fragmentation channels of multicharged proteins are and, in particular, under what circumstances protein fission and/or Coulomb explosion will be realized. In this paper we advance estimates of the Rayleigh fissibility parameter, Eq. (1), for model systems that mimic the characteristics of multicharged globular proteins [61,62]. Our analysis reveals that the dominating fragmentation channel of multicharged globular proteins involves fission rather than Coulomb explosion.
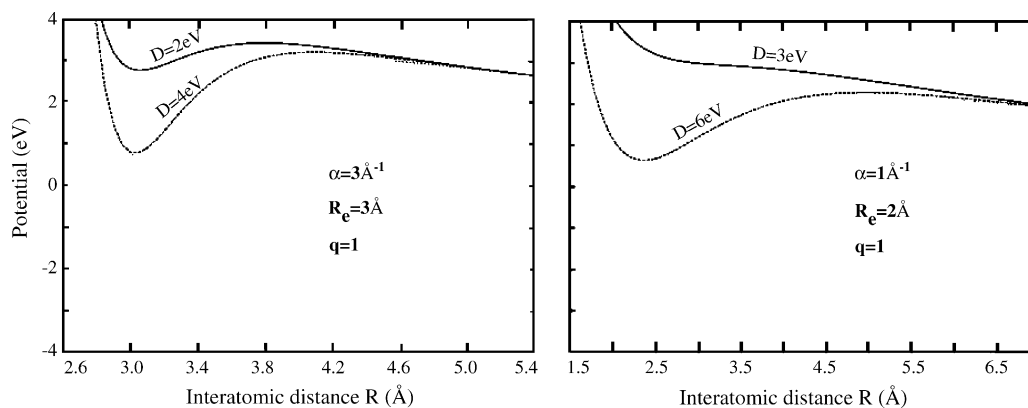
Fig. 2. Pair potentials for charged Morse clusters. The potential parameters for the (*s*) potential ($\alpha = 3\,\text{Å}^{-1}$, $R_e = 3\,\text{Å}$, $q = 1$) and for the (*ℓ*) potential ($\alpha = 1\,\text{Å}^{-1}$, $R_e = 2\,\text{Å}$, $q = 1$) are marked on the panels. The dissociation energy parameters are marked on the curves.

2. Energetics of multicharged clusters

Following our previous work [48–50] we consider the energetics of multicharged $(A^+)_n$ ($n = 55, 135, 321$) Morse clusters. The mass of each A^+ ion is 100 amu, its charge is $q = 1$, and the total cluster charge is $Z = n$. The interionic pair-potential $U(R)$ consists of an attractive Morse potential and of Coulomb repulsion:

$$U(R) = DG(G - 2) + Bq^2/R \qquad (2)$$

where

$$G = \exp[-\alpha(R - R_e)] \qquad (3)$$

D is the dissociation energy, α the range parameter, R_e is the Morse potential equilibrium distance, and $B = 14.4\,\text{eV/Å}$. Two sets of Morse potential parameters were used—(*s*): A short-range Morse potential with $D = 1–10\,\text{eV}$, $\alpha = 3\,\text{Å}^{-1}$, and $R_e = 3\,\text{Å}$ ($\alpha R_e = 9$, so that the interaction between non-neighboring atoms is negligibly small); (*ℓ*): A long-range Morse potential, with $D = 1–10\,\text{eV}$, $\alpha = 1\,\text{Å}^{-1}$, and $R_e = 2\,\text{Å}$ ($\alpha R_e = 2$, so that the contribution of interactions between non-neighboring atoms is of significance). Pair potentials for charged Morse clusters are presented in Fig. 2. The initial $t = 0$ nuclear configuration of the multicharged cluster is presented in the icosohedral geometry of the low temperature ($T = 10\,\text{K}$) cluster. A thermal, Maxwell distribution of the ion velocities was obtained after an equilibration time of 1000 fs at the low temperature.

The total potential energy $E(\{R_{ij}\})$ of the multicharged $(A^+)_n$ clusters is

$$E(\{R_{ij}\}) = \sum_{i<j} \sum U(R_{ij}) \qquad (4)$$

where the pair potentials $U(R_{ij})$ are given by Eqs. (2) and (3). $E(\{R_{ij}\})$ is presented in Fig. 3 as a function of the interatomic distances R_{ij} ($i, j = 1, \ldots, n$), where we took $R_{ij} = R$ for all nearest-neighbor distances i and j. The potential energy landscapes were calculated per atom:

$$\varepsilon(\{R_{ij}\}) = E(\{R_{ij}\})/n \qquad (5)$$

An energetically stable configuration of the $(A^+)_n$ cluster will exist, provided that its energy is negative and lower than the energy of the products in any decay channel, i.e., evaporation, fragmentation, etc. The $(A^+)_n$ clusters may also exist in a metastable configuration, with E being higher than the total energy of the products in some decay channels, but separated from them by a barrier (Fig. 3). In particular, the energy of the metastable configuration of clusters is positive, i.e., $E > 0$ (Fig. 3). To consider the stability or metastability of a cluster we introduce a limiting value $D_L(\alpha, R_e, n)$ for the dissociation energy in the pair potential, which provides a stable or metastable configuration of the $(A^+)_n$ cluster for $D > D_L(\alpha, R_e, \alpha)$. In the case of (*s*) pair potentials we find limiting values of $D_L = 4.2\,\text{eV}$ for $n = 55$, $D_L = 8.1\,\text{eV}$ for $n = 135$, and $D_L = 14.2\,\text{eV}$ for $n = 321$. In the case of (*ℓ*) pair potentials, the limiting values are $D_L = 6.5\,\text{eV}$ for $n = 55$, $D_L = 8.2\,\text{eV}$ for $n = 135$, and $D_L = 9.6\,\text{eV}$ for $n = 321$. For the case of the (*s*) pair potential the size dependence of the limiting value is of the form $D_L \propto n^{2/3}$. In the case of the (*ℓ*) pair potential, the dependence of D_L on n is considerably weaker than for the (*s*) case. All the cluster potential energies of equilibrium configurations at a minimum energy of $D > D_L$ for the potential parameters of classes (*s*) and (*ℓ*), which are presented in Fig. 3, are positive ($E > 0$), corresponding to a metastable state.

3. The liquid drop model for the cluster energetics

The potential energies of $\varepsilon = \varepsilon(\{R_{ij}^0\})$ and the multicharged metastable $(A^+)_n$ clusters ($n = 55, 135, 321$) at the metastable state, which correspond to the minimum of the potential surface (at the equilibrium configuration $\{R_{ij}^0\}$), were analyzed by the liquid drop model (LDM) [21,48,49,63]. The potential energy ε (per particle) is

$$\varepsilon = \varepsilon_C + \varepsilon_M \qquad (6)$$

where

$$\varepsilon_C = a_C n^{2/3} \qquad (7)$$

is the Coulomb energy. The Morse energy is

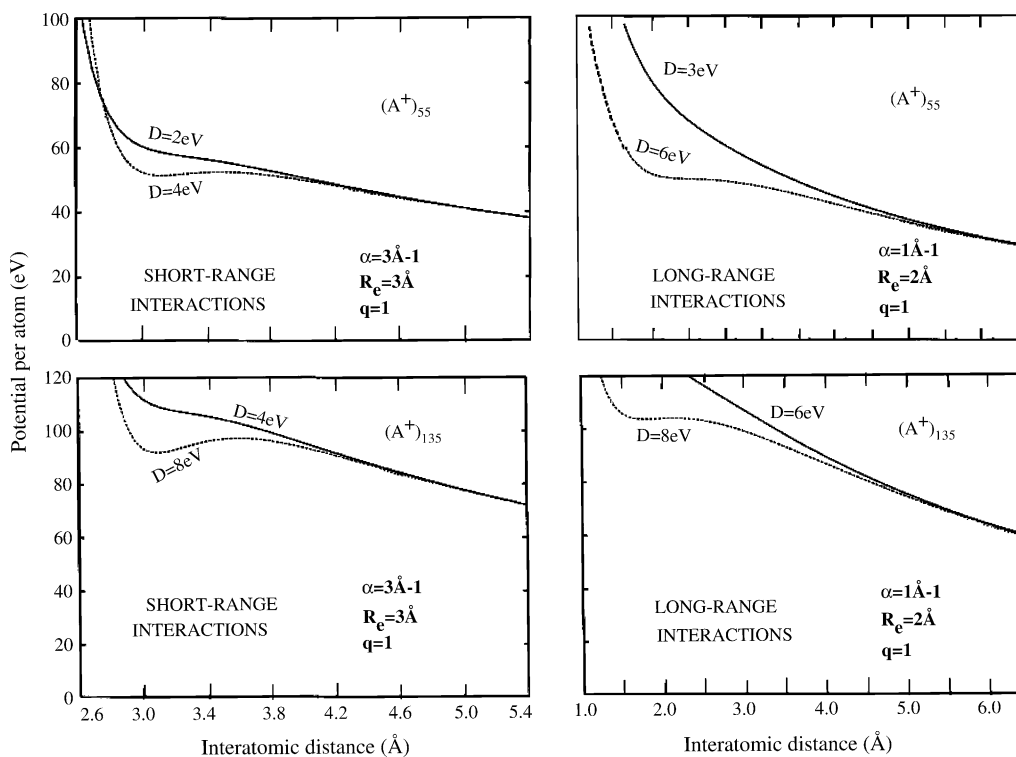$$\varepsilon_M = \varepsilon_s + \varepsilon_v \qquad (8)$$

Fig. 3. Energy landscapes for the radial expansion of $(A^+)_{55}$ clusters (the two top panels) and of $(A^+)_{135}$ clusters (the two bottom panels). The potential parameters for (s) and (ℓ) pair potentials are marked on the panels. The dissociation energy parameters are marked on the curves. Note that all the minima in the potential surfaces correspond to metastable states.
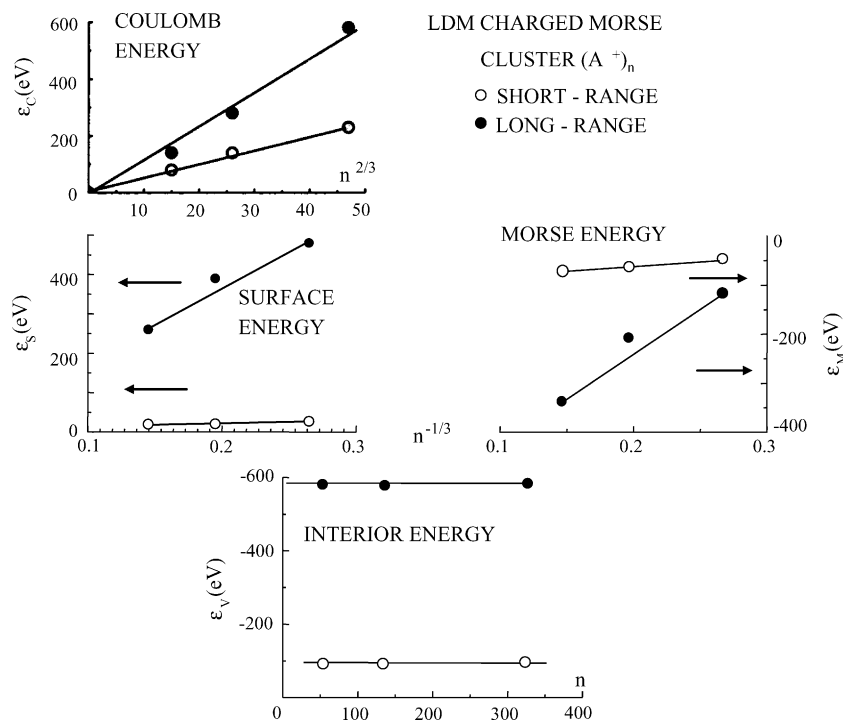

Fig. 4. Analyses of the energetics of the icosohedral charged $(A^+)_n$ ($n = 55, 135, 321$) Morse clusters by the LDM. The potential parameters are: (s) short-range potential with $\alpha = 3\,\text{Å}^{-1}$, $R_e = 3\,\text{Å}$, $D = 14.2\,\text{eV}$ and $q = 1$ ($\bigcirc$); (ℓ) long-range potential with $\alpha = 1\,\text{Å}^{-1}$, $R_e = 2\,\text{Å}$, $D = 9.6\,\text{eV}$ and $q = 1$ ($\bullet$). All energies are given per particle.

where the surface energy is $\varepsilon_s = a_s n^{-1/3}$, while the interior energy is $\varepsilon_v = a_v$. Eq. (6) is then given in the form:

$$\varepsilon = a_C n^{2/3} + a_v + a_s n^{-1/3} \tag{9}$$

Here the LDM parameters a_C, a_v and a_s are size independent. Model calculations of the cluster size dependence of the energies ε_C, ε_s and ε_v are presented in Fig. 4 for (s)-type Morse clusters with $D = 14.2$ eV and for (ℓ)-type Morse clusters with $D = 9.6$ eV. These high D parameters correspond to the D_L limiting values for the largest size ($n = 321$) clusters. The LDM scaling laws, $\varepsilon_C \propto n^{2/3}$, $\varepsilon_s = n^{-1/3}$ and $\varepsilon_v = $ const, are obeyed (Fig. 4).

The dependence of the total energy ε, Eq. (9), and the LDM parameters on the Morse potential dissociation energy D, was explored [49]. On the basis of our previous analysis [49] we assert that a_C is independent on D, while parameters a_v and a_s exhibit a linear dependence on D, i.e., $a_v = a_v^0 D$ and $a_s = a_s^0 D$. The cluster size dependence of ε can then be represented in the form:

$$\varepsilon = a_C n^{2/3} + D(a_v^0 + a_s^0 n^{-1/3}) \tag{10}$$

where a_C, a_v^0 and a_s^0 are independent of D and depend on the Morse pair-potential parameters α and R_e.

In Table 1, we present the LDM parameters a_C, a_v^0 and a_s^0 for the (s)-type and for the (ℓ)-type Morse clusters. An additional important structural attribute for the energy landscape is the equilibrium bond length r_0. From the energy landscapes (Fig. 3) we infer that for the bond dissociation energies of chemical interest ($D = 2$–6 eV) characteristic bond lengths are $r_0 = 3$ Å for the (s)-type potential and $r_0 = 1.5$ Å for the (ℓ)-type potential. For the (s)-type potential $r_0 \sim R_e$, with the bond length in the cluster being close to the minimum of the pair potential, while for the (ℓ)-type potential $r_0 > R_e$. The bond lengths manifest a weak cluster size dependence in the $n = 55$–321 domain. From the data of Table 1 we infer that the three LDM parameters a_C, a_v^0 and a_s^0 for the (ℓ)-type cluster are larger than for the (s)-type cluster. The parameter a_C is larger by a numerical factor of ~ 2 for the (ℓ)-type cluster than for the (s)-type cluster, obeying the relation $a_C \propto (r_0)^{-1}$, which is in accord with the basic expression for the cluster charging energy. The a_v^0 parameter is larger by a numerical factor of ~ 7 for the (ℓ)-type cluster than for the (s)-type cluster. We expect that the volume energy parameter is determined by the Morse potential range at the equi-

librium cluster configuration. Indeed, a_v^0 obeys the approximate relation $a_v^0 \propto (\alpha r_0)^{-1}$. Finally, the a_s^0 parameter is larger by a numerical factor of ~ 12 for the (ℓ)-type cluster relative to the (s)-type cluster, obeying the empirical energy $a_s^0 \propto (\alpha r_0)^{-3/2}$. From these results, the energies of the multicharged Morse clusters, Eq. (10), can be expressed in the form:

$$\varepsilon = \bar{a}_C^0 (1/r_0) n^{2/3} + \bar{a}_v^0 (D/\alpha r_0) + \bar{a}_s^0 D (1/\alpha r_0)^{3/2} n^{-1/3} \tag{11}$$

with the reduced LDM parameters

$$\bar{a}_C^0 = a_C r_0, \qquad \bar{a}_v^0 = a_v (\alpha r_0/D) = a_v^0 (\alpha r_0),$$
$$\bar{a}_s^0 = a_s (\alpha r_0)^{3/2}/D = a_s^0 (\alpha r_0)^{3/2} \tag{11a}$$

being given in Table 1. The reduced LDM parameters, $\bar{a}_C^0$, $\bar{a}_v^0$, and $\bar{a}_s^0$, Eq. (11a), are independent of the Morse pair-potential parameters. It is instructive to note that each of these reduced LDM parameters for the (s) and the (ℓ) clusters (Table 1) are nearly identical (within 20%), being independent of the nature and range of the Morse potential. At this stage we can discard the segregation between (s)-type and (ℓ)-type potentials and use Eq. (11) for the characterization of the energetics of Morse clusters.

4. The fissibility parameter

An important parameter, which characterizes the nature of the dominating fragmentation channel of a multicharged cluster, is the fissibility parameter, Eq. (1). On the basis of the LDM analysis of Section 3, the fissibility parameter for a $(A^{n+})_n$ cluster is given by

$$X = \varepsilon_C / 2\varepsilon_s \tag{12}$$

From Eqs. (7) and (8) we obtain:

$$X = (a_C/2a_s) n \tag{13}$$

It follows from Eq. (13) that for the fragmentation of the $(A^+)_n$ cluster $X \propto n$. In the more general case of the fragmentation of a $(A_n)^{Z+}$ cluster of size n and total charge Z (for $Z \gg 1$), n in Eq. (13) should be replaced by Z^2/n, whereupon $X \propto (Z^2/n)$. Accordingly, we replace Eq. (13) by

$$X = (a_C/2a_s)(Z^2/n) \tag{14}$$

From the preceding analysis, which led to Eq. (11), we infer that $a_C = \bar{a}_C^0 (D/r_0)$ and $a_s = \bar{a}_s^0 D/(\alpha r_0)^{3/2}$. Accordingly, the fissibility parameter, Eq. (14), will be given by

$$X = (\bar{a}_C^0/2\bar{a}_s^0)(\alpha^{3/2} r_0^{1/2}/D)(Z^2/n) \tag{15}$$

Finally, the fissibility parameter can be expressed in the form which is common in nuclear physics and in metal cluster physics [21,63], i.e.,

$$X = (Z^2/n)/(Z^2/n)_{cr} \tag{16}$$

where

$$(Z^2/n)_{cr} = (2\bar{a}_s^0/\bar{a}_C^0)(D/\alpha^{3/2} r_0^{1/2}) \tag{17}$$

Eq. (16) represents the ratio between surface and Coulomb energies on the single constituent scale. With an uncertainty range

Table 1

Parameters for the LDM fit of the equilibrium potential energies for icosohedral $(A^+)_n$ clusters ($n = 55, 135, 321$)

Potential	(s) $\alpha = 3$ Å^{-1}; $R_e = 3$ Å	(ℓ) $\alpha = 1$ Å^{-1}; $R_e = 1$ Å
a_C (eV)	4.8	10.8
$\bar{a}_C^0$ (eV Å)	14.4	16.2
a_v^0	−6.9	−50
$\bar{a}_v^0$	−62	−75
a_s^0	11.5	148
$\bar{a}_s^0$	310	280
r_0 (Å)	3.0	1.5

The nature of the potential ((s) or (ℓ)) is specified in the columns. Data for a_C, $\bar{a}_C^0$ and $\bar{a}_s^0$ from Ref. [49].

of $\pm 10\%$ the data of Table 1 result in $2\bar{a}_s^0/\bar{a}_C^0 \cong 47$. For multi-charged large molecules and biomolecules we shall specify the Coulomb instability by Eq. (16) with

$$(Z^2/n)_{cr} = 47D/\alpha^{3/2}r_0^{1/2} \tag{18}$$

The parameters units in Eqs. (17) and (18) are: $(\bar{a}_C^0$ (eV Å)), $(D$ (eV)), $(\alpha$ (Å^{-1})) and $(r_0$ (Å)).

5. On the Coulomb instability of multicharged proteins

We would like to inquire what the fragmentation pattern of multicharged proteins in the gas phase is. In particular, it is of considerable interest whether multicharged "isolated", anhydrous protein fission or Coulomb explosion occurs. This issue is of importance in the context of the mass-spectrometric interrogation of highly charged polypeptides and proteins in the gas phase.

We shall apply Eqs. (16) and (18) for the fissibility parameter to specify the fragmentation pattern of multicharged globular proteins [61,62]. In spite of its simplicity, we expect that our model (Section 4) for the Coulomb stability of Morse clusters will provide guidelines for the characterization of the fragmentation patterns of spherical polypeptides and globular proteins. The size n for such biomolecules is specified in terms of the number of residues, while the total charge is taken from mass-spectrometry, resulting in the value of Z^2/n. To characterize the normalization parameter $(Z^2/n)_{cr}$, Eq. (18), we choose the Morse potential parameters D, α and r_0, and the typical values corresponding to chemical C–H, N–H, C–N and C=O bonds, which fall in the range $r_0 = 1.1$–1.4 Å, $\alpha = 2.0$–2.3 Å^{-1} and $D = 3.5$–11 eV. For the sake of a rough estimate we take average values of $D = 6$ eV, $\alpha = 2.2$ Å^{-1} and $r_0 = 1.2$ Å, and estimate from Eq. (18) that $(Z^2/n)_{cr} \simeq 79$. From this heuristic numerical analysis we infer that protein fission (for $X < 1$) will prevail when

$$Z^2/n < 79 \tag{19a}$$

while protein Coulomb explosion (for $X > 1$) occurs when

$$Z^2/n > 79 \tag{19b}$$

From Eqs. (19a) and (19b) we infer that large values of Z^2/n are required to induce Coulomb explosion, while for small values of Z^2/n fission will be realized. Typical values of n and Z currently available for globular proteins [61,62] correspond to rather low values of Z^2/n. For cytochrome C [61] $n = 104$ and $Z = 8$–19 ($Z^2/n = 0.5$–4), for carbonic anhydrase [61,62] $n = 260$ and $Z = 45$ ($Z^2/n = 7$), while for G-actin [61] $n = 370$ and $Z = 59$ ($Z^2/n = 9$). For these proteins, the fissibility parameters X, Eq. (16), are low, falling in the range $X = 6 \times 10^{-3}$ to 0.1. Accordingly, the fragmentation pattern of multicharged proteins involves spatially anisotropic protein fission into a small number of large fragments with relatively low kinetic energies (i.e., $E_{KIN}/E_{IN} \ll 1$). Protein fission is expected to involve a thermally activated process over a high potential barrier, which is roughly estimated to be $E_{BARRIER} \simeq 0.5$ eV, in analogy with our analysis of the activation energy in the fragmentation dynamics of multicharged Morse clusters [50]. The existence of the fission fragmentation

channel with a high barrier will insure the structural integrity of proteins in mass-spectrometric experiments. Kinetic energy release studies of the melittin peptide with $Z = 3$ and $n = 36$, which are characterized by a low value of $Z^2/n = 0.3$, reveal energetic ionic dissociation with the production of several small fragments (energies of 1.25 eV), presumably induced by local Coulomb repulsion effects in this moderately small peptide. Our work provided guidelines for the characterization of the gross features of protein fission and Coulomb explosion. Further experimental mass-spectrometric studies and computational studies of Coulomb instability of peptides and proteins are called for.

6. Epilogue

Our interest in the Coulomb instability and fragmentation dynamics of highly charged proteins was inspired by conversations of one of us (JJ) with Chava Lifshitz about protein mass-spectrometry. This article is dedicated to the memory of Chava Lifshitz, a wonderful person, a remarkable educator and an outstanding scientist.

References

[1] K. Sattler, J. Mühlbach, O. Echt, P. Pfau, E. Recknagel, Phys. Rev. Lett. 47 (1981) 160.
[2] D. Kreisle, O. Echt, M. Knapp, E. Recknagel, K. Leiter, T.D. Märk, J.J. Sáenz, J.M. Soler, Phys. Rev. Lett. 56 (1986) 1551.
[3] P. Scheier, T.D. Märk, Chem. Phys. Lett. 136 (1987) 423.
[4] M. Lezius, T.D. Märk, Chem. Phys. Lett. 155 (1989) 496.
[5] A.J. Stace, P.G. Lethbridge, J.K.E. Upham, J. Phys. Chem. 93 (1989) 333.
[6] S. Sugaron, A. Tamura, Y. Ishii, Z. Phys. D 12 (1989) 213.
[7] C. Bréchignac, Ph. Cahuzac, J. Leygnier, J. Weiner, J. Chem. Phys. 90 (1989) 1492.
[8] M. Lezius, P. Scheier, A. Stamatovic, T.D. Märk, Chem. Phys. 91 (1989) 3240.
[9] I. Katakuse, H. Ito, A. Ichihara, Int. J. Mass Spectrom. Ion Proc. 97 (1990) 47.
[10] C. Bréchignac, Ph. Cahuzac, F. Carliez, M. de Frutos, Phys. Rev. Lett. 64 (1990) 2893.
[11] W.A. Saunders, N. Dam, Z. Phys. D 20 (1991) 111.
[12] C. Bréchignac, Ph. Cahuzac, N. Kebaili, J. Leignier, A. Sarfati, Phys. Rev. Lett. 68 (1992) 3916.
[13] N.G. Gotts, P.G. Lethbridge, A.J. Stace, J. Chem. Phys. 96 (1992) 408.
[14] H.J. Krappe, Z. Phys. D 23 (1992) 269.
[15] W.A. Saunders, Phys. Rev. A 46 (1992) 7028.
[16] C. Bréchignac, Ph. Cahuzac, F. Carlier, M. de Frutos, Phys. Rev. B 49 (1994) 2825.
[17] A. Goldberg, I. Last, T.F. George, J. Chem. Phys. 100 (1994) 8277.
[18] U. Näher, S. Frank, N. Malinowski, U. Zimmermann, T.P. Martin, Z. Phys. D 31 (1994) 191.
[19] F. Chandezon, C. Guet, B.A. Huber, M. Jalabert, E. Maurel, E. Monnand, C. Ristori, J.C. Rocco, Phys. Rev. Lett. 74 (1995) 3784.

[20] C. Bréchignac, Ph. Cahuzac, M. de Frotos, N. Kebaili, A. Sarfati, Phys. Rev. Lett. 77 (1996) 251.

[21] U. Näher, S. Bjornholm, S. Fraundorf, F. Gracias, C. Guet, Phys. Rep. 285 (1997) 245.

[22] C. Guet, X. Biquard, P. Blaise, S.A. Blundell, M. Gross, B.A. Huber, D. Jalabert, M. Maurel, L. Plague, J.C. Rocco, Z. Phys. D 40 (1997) 317.

[23] O. Shapiro, P.J. Kunz, K. Möhring, P.A. Hervieux, D.H.F. Gross, M.E. Madjet, Z. Phys. D 41 (1997) 219.

[24] C. Bréchignac, Ph. Cahuzac, N. Kébaili, J. Leygnier, Phys. Rev. Lett. 81 (1998) 4612.

[25] N. Saito, K. Koyama, M. Tanimoto, Chem. Phys. Lett. 300 (1999) 262.

[26] J. Purnell, E.M. Snyder, S. Wei, A.W. Castleman Jr., Chem. Phys. Lett. 229 (1994) 333.

[27] O. Zhong, A.W. Castleman Jr., Chem. Rev. 100 (2000) 4039.

[28] T. Ditmire, T. Donnelly, A.M. Rubenchik, R.W. Falcone, M.D. Perry, Phys. Rev. A 64 (1996) 3379.

[29] T. Ditmire, J.W.G. Tisch, E. Springate, M.B. Mason, N. Hay, R.A. Smith, J. Marangos, M.H.R. Hutchinson, Nature (London) 386 (1997) 54.

[30] T. Ditmire, J.W.G. Tisch, E. Springate, M.B. Mason, N. Hay, J.P. Marangos, M.H.R. Hutchinson, Phys. Rev. Lett. 78 (1997) 2732.

[31] M.H.R. Hutchinson, T. Ditmire, E. Springate, J.W.G. Tisch, Y.L. Shao, M.B. Mason, N. Hay, J.P. Marangos, Philos. Trans. R. Soc. London, Ser. A 356 (1998) 297.

[32] T. Ditmire, E. Springate, J.W.G. Tisch, Y.L. Shao, M.B. Mason, N. Hay, J.P. Marangos, M.H.R. Hutchinson, Phys. Rev. A 57 (1998) 369.

[33] E. Springate, N. Hay, J.W.G. Tisch, M.B. Mason, T. Ditmire, M.H.R. Hutchinson, J.P. Marangos, Phys. Rev. A 61 (2000) 063201.

[34] J. Kou, N. Nakashima, S. Sakabe, S. Kawato, H. Ueyama, T. Urano, T. Kuge, Y. Izawa, Y. Kato, Chem. Phys. Lett. 289 (1998) 334.

[35] V.P. Krainov, M.B. Smirnov, Phys. Rep. 370 (2002) 237.

[36] M. Lezius, S. Dobosh, D. Normand, M. Schmidt, Phys. Rev. Lett. 80 (1998) 261.

[37] J. Daligault, C. Guet, Phys. Rev. A 64 (2001) 043203.

[38] F. Chandezon, S. Tomita, D. Cornier, P. Grubling, C. Guet, H. Lebius, A. Pesnelle, B.A. Huber, Phys. Rev. Lett. 87 (2001) 153402.

[39] F. Chandezon, T. Bergen, A. Brenac, C. Guet, B.A. Huber, H. Lebius, A. Pesnelle, Phys. Rev. A 63 (2001) 051201.

[40] I. Last, I. Schek, J. Jortner, J. Chem. Phys. 107 (1997) 6685.

[41] I. Last, J. Jortner, Phys. Rev. A 60 (1999) 2215.

[42] I. Last, J. Jortner, Phys. Rev. A 62 (2000) 013201.

[43] I. Last, J. Jortner, J. Chem. Phys. 120 (2004) 1336.

[44] I. Last, J. Jortner, J. Chem. Phys. 120 (2004) 1348.

[45] I. Last, J. Jortner, J. Chem. Phys. 121 (2004) 8329.

[46] I. Last, J. Jortner, Proc. Natl. Acad. Sci. U.S.A. 102 (2005) 1291.

[47] I. Last, J. Jortner, Phys. Rev. A 71 (2005) 063204.

[48] I. Last, Y. Levy, J. Jortner, Proc. Natl. Acad. Sci. U.S.A. 99 (2002) 9107.

[49] I. Last, Y. Levy, J. Jortner, J. Chem. Phys. 123 (2005) 154301.

[50] Y. Levy, I. Last, J. Jortner, Mol. Phys., in press.

[51] N. Bohr, J.A. Wheeler, Phys. Rev. 56 (1939) 426.

[52] L. Meitner, O.R. Frisch, Nature 143 (1939) 239.

[53] S. Frenker, N. Metropolis, Phys. Rev. 72 (1947) 914.

[54] P. Möller, D.G. Madland, A.J. Sierk, A. Iwamoto, Nature (London) 409 (2001) 785.

[55] L. Lord Rayleigh, Phil. Mag. 14 (1884) 184.

[56] D.C. Taflin, T.I. Ward, E.J. Davis, Langmuir 5 (1989) 376.

[57] J.F. Widman, C.L. Arrdahl, E.J. Davis, Aerosol Sci. Technol. 27 (1979) 636.

[58] D. Duft, H. Lebius, B.A. Huber, C. Guet, T. Leisner, Phys. Rev. Lett. 89 (2002) 084503.

[59] L. Pruvost, I. Serri, H.T. Duong, J. Jortner, Phys. Rev. A 61 (2000) 053408.

[60] J. Jortner, M. Rosenblit, Adv. Chem. Phys. 132 (2005) 247.

[61] S. Cherokee, A. Hoaglund-Hyser, E. Counterman, D.E. Clemmer, Chem. Rev. 99 (1999) 3037.

[62] J. Laskin, C. Lifshitz, J. Mass Spectrom. 36 (2001) 459.

[63] P. Heyde, Basic Ideas and Concepts in Nuclear Physics, Institute of Physics Publishing, Bristol, 1994.